DOI: 10.1002/chem.200901708

Au Nanowire–Au Nanoparticles Conjugated System which Provides Micrometer Size Molecular Sensors

Taejoon Kang, Ilsun Yoon, Jangbae Kim, Hyotcherl Ihee, and Bongsoo Kim*[a]

Abstract: We report a new type of molecular sensor using a Au nanowire (NW)–Au nanoparticles (NPs) conjugated system. The Au NW–NPs structure is fabricated by the self-assembly of biotinylated Au NPs on a biotinylated Au NW through avidin; this creates hot spots between NW and NPs that strongly enhance the Raman signal. The number of the Au NPs attached to the NW is reproducibly proportional to the concentration of the avidin, and is also proportional to the measured surface-enhanced Raman scattering (SERS) signals. Since this well-defined NW–NPs conjugated sensor is only a few micrometer long, we expect that development of multiplex nanobiosensor of a few tens micrometer size would become feasible by combining individually modified multiple Au NWs together on one substrate.

Keywords: biosensors · gold · nanomaterials · nanowires · surface-enhanced raman scattering

Introduction

Metal–metal nanostructures with a very small gap at the junction can play important roles in the development of efficient bio/chemical sensors via surface-enhanced Raman scattering (SERS),[1] since they provide a region of very intense electromagnetic fields, "hot spots", in the metal gap.[2] In the hot spot areas, the Raman signal of molecules is greatly increased, allowing the detection of even a single molecule under ambient condition.[3] Furthermore, SERS spectra provide a signature for specific chemical groups that can be used for the identification of analytes.[4]

Noble metal nanoparticles (NPs) and nanowires (NWs) are two important elementary nanostructures that have attracted great interest as SERS-active platforms because of their well-defined geometry and simple fabrication.[5] A number of NP-based nanostructures have been fabricated,[6] and SERS-sensors employing metal nanowires have been also developed such as a single NW on a film (SNOF) and NW pairs.[7] Recently, a SERS-active system combining a NW and NPs have attracted much attention. While many interesting optical properties of these nanostructures such as polarization dependence and remote excitation of SERS signals were observed,[8b–e] molecular sensors employing this NW–NPs structure have not been successfully fabricated yet.

Herein, we report a new biomolecule detection method using a Au NW–Au NPs conjugated system. We found that the concentration of a target molecule can be reproducibly determined from the number of NPs attached on the NW as well as the SERS intensity. Furthermore, this sensor can be fabricated into the size of a few micrometers because it employs only a single Au NW. We expect that a multiplex biomolecule sensor of a size of tens of micrometers could be constructed by combining individually functionalized multiple Au NWs.

The well-studied biotin–avidin system with a high binding affinity ($K_a \sim 10^{13}\,\text{M}^{-1}$) is selected for the detection test (Figure 1). Since avidin, a tetrameric protein, can bind up to biotinylated molecules (i.e., antibodies, inhibitors, DNA) with minimal impact on its biological activity,[9] the detection of avidin provides a convenient and practical pathway for extending the analyte accessibility of biosensor. The Au NW and NPs modified with biotin were self-assembled upon the addition of avidin to the solution and NW–NPs conjugated systems were formed. These self-assembled Au NW–NPs structures were visualized by scanning electron microscope (SEM) and also confirmed by SERS measurements (Figure 2). The biomolecule sensing through this NW–NPs conjugated system retains high selectivity and label-free detection. SERS spectra were obtained over the concentration range $10^{-13}\,\text{M} < [\text{avidin}] < 10^{-5}\,\text{M}$.

[a] T. Kang, Dr. I. Yoon, J. Kim, Prof. H. Ihee, Prof. B. Kim
Department of Chemistry, KAIST
Daejeon, 305-701 (Korea)
Fax: (+82) 42-350-2810
E-mail: bongsoo@kaist.ac.kr

Results and Discussion

Fabrication of Au NW–NPs structure is based on self-assembly of Au NPs to an atomically smooth surface of a Au NW through biotin–avidin interaction. Hot spots are generated at Au NW–NPs junctions and the target molecules are collocated in these hot spot regions. Figure 1 shows a schematic representation of a self-assembled Au NW–NPs structure. Au NPs (~10 nm diameter) were purchased and Au NWs (~150 nm diameter) were synthesized on a *c*-sapphire substrate by a vapor transport method.[7a,b] The Au NWs are single-crystalline and have atomically flat facets. The surfaces of Au NWs were modified in the stock solution of EZ-Link biotin HPDP[9d] and rinsed by excess of solvents. In a similar manner, Au NPs were functionalized by adding 2 μL of a 0.4 mM stock solution of EZ-Link Biotin HPDP in NPs solution. The biotinylated Au NWs were incubated in an avidin solution first and then immersed into a biotinylated Au NPs solution to fabricate Au NW–NPs structures through the binding of biotin and avidin. After washing to remove non-specifically bound NPs, the SEM and SERS measurements were carried out.

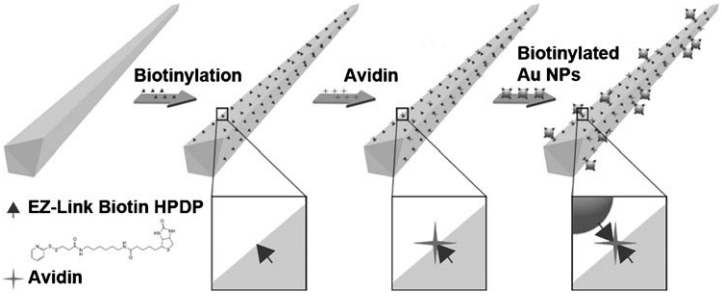

Figure 1. Schematic illustration for the detection of avidin by the bioconjugated Au NW–NPs system. Au NPs were captured on a Au NW by biotin–avidin recognition, resulting in the creation of a SERS-active Au NW–NPs structure. The chemical structure of the EZ-Link Biotin HPDP is shown.

Figure 2a shows the SEM image of a typical Au NW–NPs structure assembled by biotin–avidin interaction. The NPs are clearly discerned, densely attached, and evenly distributed over the whole Au NW without aggregated NPs. Thus these conjugated NW–NPs can provide strong SERS spectra with an intensity proportional to the avidin concentration. Few NPs were observed, on the other hand, on the NW surface when the self-assembly of NPs and NW were performed using pure phosphate-buffered saline (PBS) solution without avidin (Figure 2b). This shows that the Au NW–NPs structure can be formed only in the presence of avidin.

A strong SERS signal is observed from the Au NW–NPs conjugated system assembled in the presence of avidin (upper spectrum in Figure 3a) and featureless spectrum except for a weak Si band is obtained when the biotinylated Au NW is exposed to biotinylated NPs in the absence of avidin (lower spectrum in Figure 3a). The SERS spectra

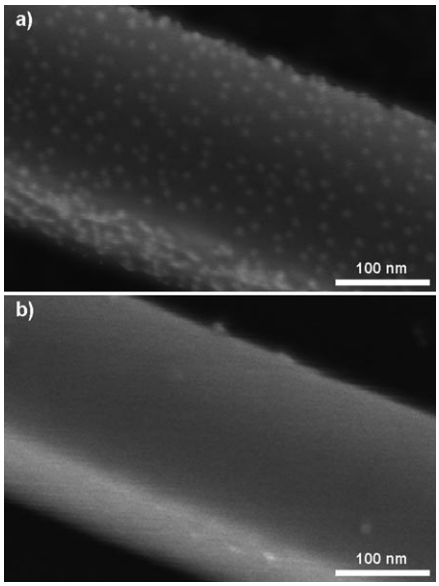

Figure 2. SEM images of a) Au NW–NPs system by biotin–avidin interaction with avidin concentration of 10^{-6} M and b) non-specifically bound Au NPs onto Au NW without avidin. Evenly distributed Au NPs are clearly seen in a), while few Au NPs are identified in b).

were measured at the midsection of Au NW–NPs system and the laser polarization was perpendicular to the long axis of NW. This result is consistent with the observations in micrographs of Figure 2. The SERS signal is not enhanced in the absence of NPs attached on the NW because it is very hard to excite surface plasmon of Au NW without the NP.[7a] The enhanced SERS signal obtained from Au NW–NPs structure verifies that the coupling between NW and NP generates a hot spot and also suggests that a single NW–NPs conjugated structure can be employed as a SERS sensor for biomolecule detection.

The SERS spectrum of a Au NW–NPs structure shows several Raman bands from 1000 to 1600 cm^{-1}, originating from EZ-Link Biotin HPDP molecules captured in the gap between the NW and NPs. The Raman spectrum obtained from EZ-Link Biotin HPDP in solid state shows an identical Raman spectrum. These Raman bands are mainly attributed to the pyridyl group of EZ-Link Biotin HPDP because the SERS spectrum in Figure 3a is quite similar to the reported spectra of pyridinethiol.[10] In this experiment, the pyridyl group plays a role as a label for enhanced Raman signal.

We have estimated the enhancement factor (EF) by the formation of Au NW–NPs structure through the following equation:[11]

$$EF = (I_{SERS} \times N_{bulk})/(I_{bulk} \times N_{SERS})$$

where I_{SERS} and I_{bulk} are the peak intensities for the SERS and bulk spectra of the 1005 cm^{-1} band, N_{bulk} is the number of molecules contributing to a bulk spectrum, and N_{SERS} is the number of molecules at the hot spot regions. N_{bulk} was determined based on the focal volume of our Raman system

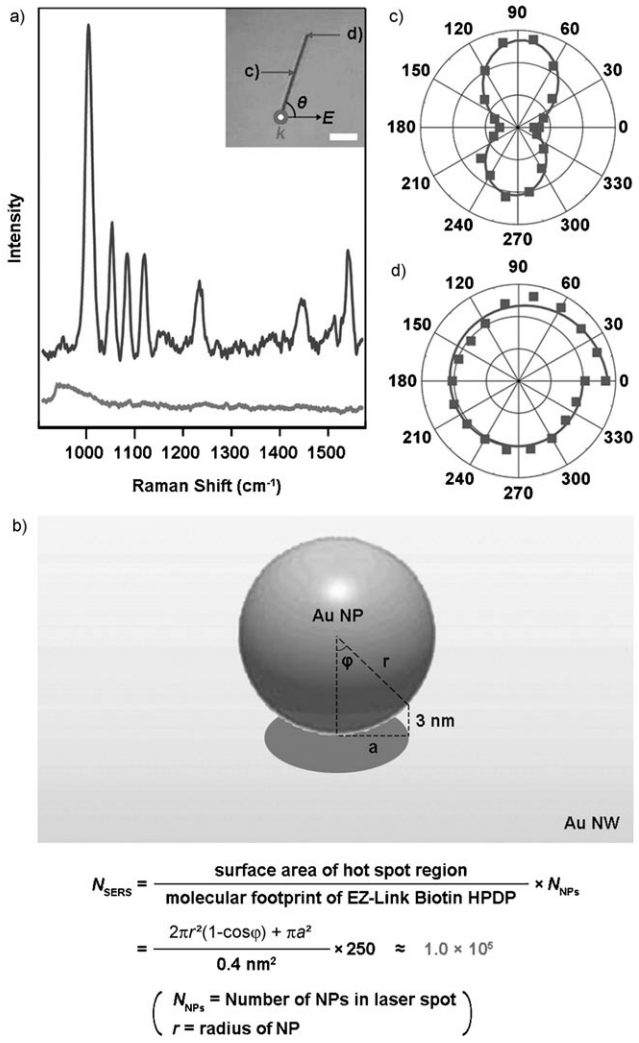

$$N_{SERS} = \frac{\text{surface area of hot spot region}}{\text{molecular footprint of EZ-Link Biotin HPDP}} \times N_{NPs}$$

$$= \frac{2\pi r^2(1-\cos\varphi) + \pi a^2}{0.4\ \text{nm}^2} \times 250 \approx 1.0 \times 10^5$$

(N_{NPs} = Number of NPs in laser spot; r = radius of NP)

Figure 3. a) SERS spectra obtained from the bioconjugated Au NW–NPs structure (upper spectrum) and biotinylated Au NW exposed to biotinylated Au NPs in the absence of avidin (lower spectrum). The inset is an optical microscope image of Au NW–NPs structure. The k and E vectors indicate the incident direction of laser light and the polarization direction. The scale bar denotes 5 μm. b) Schematic representation of the estimated hot spot region and calculating expression of N_{SERS}. c)–d) Polar plots of integrated SERS intensities of 1005 cm^{-1} Raman band with respect to θ at the center and the tip of the NW–NPs conjugated system, respectively (see inset of a).

(~0.5 femtoL) and the density of EZ-Link Biotin HPDP in solid state (~0.5 $g\,cm^{-3}$), so that N_{bulk} is about 2.8×10^8. N_{SERS} was estimated by calculating the surface area of a single Au NW–NP hot spot region, dividing it by the molecular area of a single EZ-Link Biotin HPDP, and then multiplying the number of NPs in the laser spot (~500 nm diameter). We chose the hot-spot region for which the NW–NP gap is less than 3 nm and the surface area of this hot-spot region was calculated as shown in Figure 3b. The molecular footprint of EZ-Link Biotin HPDP was assumed ~0.4 nm^2 and the number of Au NPs illuminated by the laser light was determined about 250 from Figure 2a, therefore, the calculated N_{SERS} is about 1.0×10^5. The intensity ratio of SERS from Au NW–NPs system and bulk spectrum of EZ-Link Biotin HPDP is about 94. Finally, the EF of Au NW–NPs structure was calculated to be 2.6×10^5. Note that the molecule does not have an absorption band around 633 nm. Further enhancement of the SERS intensity can be achieved by optimization of the laser wavelength to induce resonance Raman effects.

Figure 3c–d show polarization dependence of integrated SERS intensities of 1005 cm^{-1} band from the Au NW–NPs structure. At the center, the SERS intensity is maximized when the polarization is perpendicular to the NW axis and minimized when the polarization is parallel. This polarization dependence was best-fit to an $Ae^{-B\theta}\cos^2\theta + C$ function. In this expression, the exponential decay was used to describe the photobleaching induced SERS signal decrease. The surface plasmon can be excited differently at the tip and the center of the NW–NPs structure by the laser polarization. At the tip of NW–NPs system, there is a distribution of the surface angles with respect to a fixed laser polarization, leading to rather isotropic polarization angle dependence. When a single NP is attached to the midsection of a NW, strong polarization anisotropy has been observed.[8b,c] Since many NPs are self-assembled onto the NW in this experiment, the observed polarization dependence represents that of the collection of many hot spots. On the other hand, at the tip of the NW the local structure is similar to a hemisphere capping a cylinder. Hence, the polarization anisotropy disappears at the large sphere uniformly covered with small NPs. Similar polarization dependence of NW–NPs structure has been recently reported by Moskovits group.[8c]

Figure 4a exhibits the dependence of the SERS spectrum from Au NW–NPs structure on the concentration of avidin. The PBS solutions of avidin with a concentration range $10^{-13}\,M < [\text{avidin}] < 10^{-5}\,M$ were examined by the method illustrated in Figure 1. An intense SERS spectrum was obtained when the concentration of avidin was higher than $10^{-8}\,M$. At $10^{-9}\,M$, the SERS intensity became much weaker and at the concentration below $10^{-10}\,M$, Raman signal was hardly detectable. These SERS spectra agree well with the SEM images of Figure 4b in that the number of captured Au NPs increases as the concentration of avidin increases. This result clearly shows that the SERS enhancement is approximately proportional to the number of constructed NW–NP hot spots and the number of NPs attached onto NW strongly related with the concentration of avidin. Since Au NWs have atomically smooth surfaces and NPs are evenly distributed over the whole NW without aggregates, the measured SERS signals from the NW–NP structure is proportional to the number of NW–NP hot spots and nonlinearly dependent on the concentration of target avidin. The nonlinearity and apparent saturation of the SERS signal and NP density at higher concentrations are due to the finite size of the NP and could be relieved by employing smaller diameter Au NPs. The reproducible concentration dependence of SERS signals from a SERS-active platform as observed by this NW–NPs structure is considered as one of the most important properties for an optimum sensor.

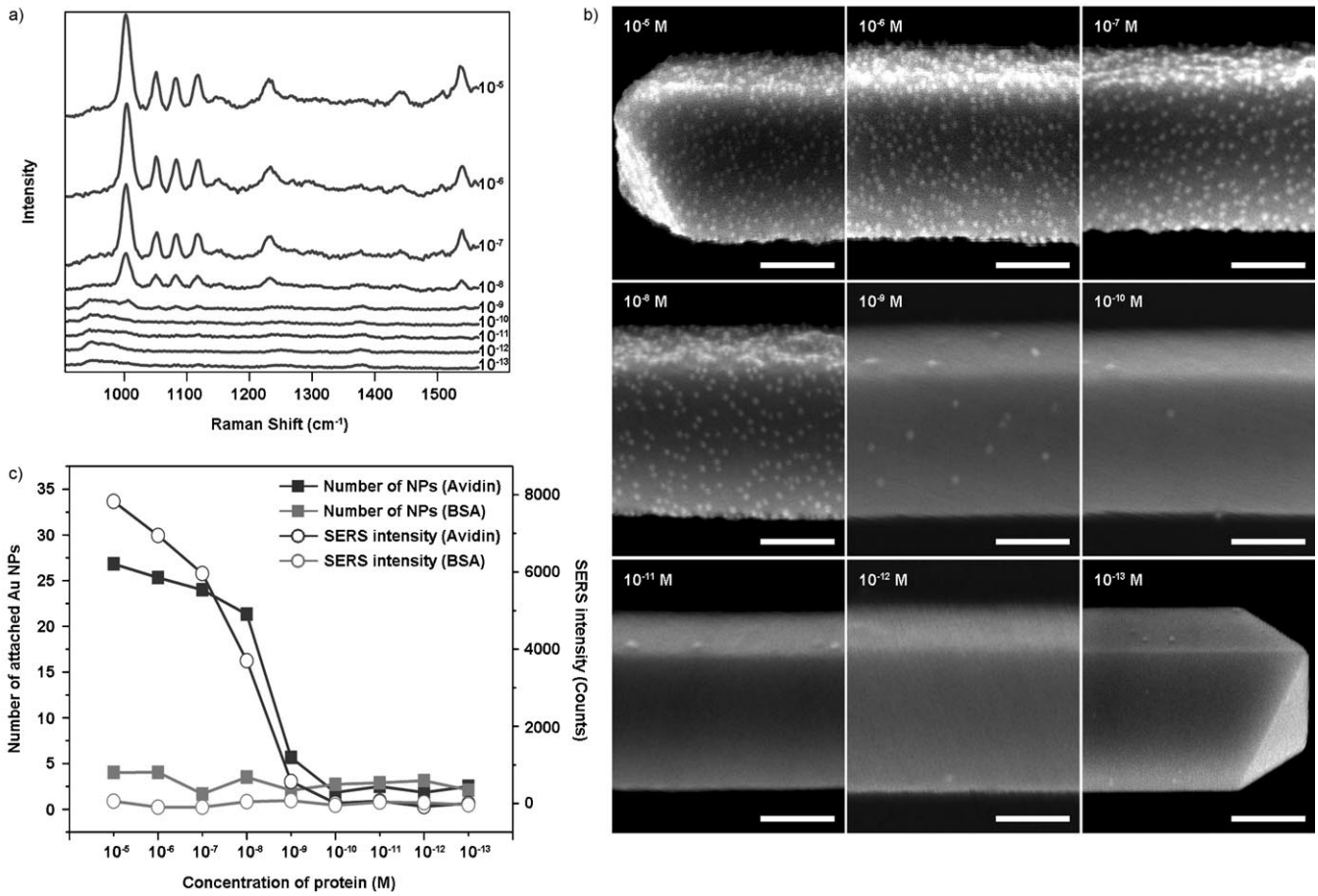

Figure 4. a)–b) SERS spectra and corresponding SEM images obtained from Au NW–NPs structure with various avidin concentrations. c) Number of attached Au NPs onto Au NW surface and SERS intensity as a function of avidin and BSA concentration.

In addition, we tried to detect a nonspecific binding protein, bovine serum albumin (BSA) instead of avidin in order to confirm that the SERS enhancement is dependent on the specific recognition of avidin. Figure 4c shows the number of Au NPs attached on the NW surface and SERS intensity versus concentration of protein curves. The number of NPs was counted from the SEM image of Au NW–NPs structure inside a surface area of $\sim 10^4$ nm^2. Self-assembled Au NW–NPs structure was not observed when the biotinylated Au NW was treated with increasing concentrations of BSA, indicating that the self-assembly leading to conjugated NW–NPs structure is highly specific for the biotin–avidin interaction.

Conclusions

In conclusion, we have demonstrated that biotinylated Au NPs were self-assembled on a biotinylated Au NW through the agency of the target avidin, creating hot spots between the NW and NPs that strongly enhance the Raman signal. By measuring SERS spectra for various concentrations of avidin and BSA, we found that label-free avidin can be detected with high sensitivity and selectivity and this single Au NW–NPs structure can be a well-defined SERS sensor. We expect that development of multiplex nanobiosensor of a few tens of micrometer in size becomes feasible by individually modifying multiple Au NWs and combining them together on one substrate.

Experimental Section

10 nm Au NPs were purchased from Sigma–Aldrich and Au NWs were synthesized on a *c*-sapphire substrate by direct evaporation of pure Au powder (99.99%, Sigma–Aldrich) which was described previously.[7a,b] The Au NWs were transferred one by one onto a Si substrate using a custom-built nanomanipulator.[7b] The Si substrates were modified with methoxy-polyethylene glycol (M-PEG) silane via a self-assembly technique before the transport of NWs.[12] The Au NWs on a Si substrate were incubated in a 4 mM stock solution of EZ-Link Biotin HPDP (Pierce) for 24 h and rinsed by excess of solvents. The Au NPs were functionalized by adding 2 μL of a 0.4 mM stock solution of EZ-Link Biotin HPDP. The mixture was shaken and allowed to set for 24 h. The unbound biotin molecules were purified away by a second round of centrifugations. The biotinylated Au NWs on a Si substrate were immersed in PBS solution of avidin (Sigma–Aldrich) for 3 h and washed by pure PBS solution. These Au NWs were incubated in biotinylated Au NPs solution for 3 h and Au NW–NPs architectures were formed by biotin–avidin interaction. The control experiment was carried out using BSA (Sigma–Aldrich) instead of avidin. The SEM images were taken on a Hitachi S-4800 oper-

ated at 10 kV. The SERS spectra were obtained with a homemade micro-Raman system based on the Olympus BX41 microscope. The 633 nm radiation of He-Ne laser (Melles Griot) was used as an excitation source and the laser light was focused on a sample through a ×100 objective (NA = 0.7, Mitutoyo). The polarization direction of laser was controlled by rotating a half-wave plate. The SERS signals were recorded with a thermoelectrically cooled electron multiplying charge coupled device (EMCCD, Andor) mounted on the spectrometer with a 1200 groove per mm grating.

Acknowledgements

This research was supported by a grant from NRL (code ROA-2007-000–20127-0), "Center for Nanostructured Materials Technology" under "21st Century Frontier R&D Programs" (code 2009K000468), Center for Intelligent Nano-Bio Materials under SRC (code R11-2005-008-03001-1-0), and Nano R&D program (code 2008-02824) of the Ministry of Education, Science and Technology, Korea.

[1] a) J. N. Anker, W. P. Hall, O. Lyandres, N. C. Shah, J. Zhao, R. P. V. Duyne, *Nat. Mater.* **2008**, *7*, 442–453; b) X. M. Qian, S. M. Nie, *Chem. Soc. Rev.* **2008**, *37*, 912–920; c) R. Gunawidjaja, S. Peleshanko, H. Ko, V. V. Tsukruk, *Adv. Mater.* **2008**, *20*, 1544–1549; d) M. L. Tran, S. P. Centeno, J. A. Hutchison, H. Engelkamp, D. Liang, G. V. Tendeloo, B. F. Sels, J. Hofkens, H. Uji-i, *J. Am. Chem. Soc.* **2008**, *130*, 17240–17241.

[2] a) M. Moskovits, *Rev. Mod. Phys.* **1985**, *57*, 783–828; b) H. Xu, E. J. Bjerneld, M. Käll, L. Börjesson, *Phys. Rev. Lett.* **1999**, *83*, 4357–4360; c) H. Xu, J. Aizpurua, M. Käll, P. Apell, *Phys. Rev. E* **2000**, *62*, 4318–4324; d) G. C. Schatz, R. P. V. Duyne in *Handbook of Vibrational Spectroscopy, Vol. 1* (Eds.: J. M. Chalmers, P. R. Griffiths), Wiley, New York, **2002**; e) H. Xu, M. Käll, *ChemPhysChem* **2003**, *4*, 1001–1005.

[3] a) S. Nie, S. R. Emory, *Science* **1997**, *275*, 1102–1106; b) K. Kneipp, H. Kneipp, I. Itzkan, R. R. Dasari, M. S. Feld, *Chem. Rev.* **1999**, *99*, 2957–2976; c) K. Kneipp, H. Kneipp, J. Kneipp, *Acc. Chem. Res.* **2006**, *39*, 443–450.

[4] a) G. A. Baker, D. S. Moore, *Anal. Bioanal. Chem.* **2005**, *382*, 1751–1770; b) H. Ko, S. Singamaneni, V. V. Tsukruk, *Small* **2008**, *4*, 1576–1599; c) H. Ko, V. V. Tsukruk, *Small* **2008**, *4*, 1980–1984.

[5] a) C. E. Talley, J. B. Jackson, C. Oubre, N. K. Grady, C. W. Hollars, S. M. Lane, T. R. Huser, P. Nordlander, N. J. Halas, *Nano Lett.* **2005**, *5*, 1569–1574; b) C. J. Murphy, T. K. Sau, A. M. Gole, C. J. Orendorff, J. Gao, L. Gou, S. E. Hunyadi, T. Li, *J. Phys. Chem. B* **2005**, *109*, 13857–13870; c) S. J. Lee, A. R. Morrill, M. Moskovits, *J. Am. Chem. Soc.* **2006**, *128*, 2200–2201; d) P. Mohanty, I. Yoon, T. Kang, K. Seo, K. S. K. Varadwaj, W. Choi, Q. H. Park, J. P. Ahn, Y. D. Suh, H. Ihee, B. Kim, *J. Am. Chem. Soc.* **2007**, *129*, 9576–9577.

[6] a) F. Svedberg, Z. Li, H. Xu, M. Käll, *Nano Lett.* **2006**, *6*, 2639–2641; b) M. Ringler, T. A. Klar, A. Schwemer, A. S. Susha, J. Stehr, G. Raschke, S. Funk, M. Borowski, A. Nichtl, K. Kürzinger, R. T. Phillips, J. Feldmann, *Nano Lett.* **2007**, *7*, 2753–2757; c) P. H. C. Camargo, M. Rycenga, L. Au, Y. Xia, *Angew. Chem.* **2009**, *121*, 2214–2218; *Angew. Chem. Int. Ed.* **2009**, *48*, 2180–2184; d) Y. Lu, G. L. Liu, L. P. Lee, *Nano Lett.* **2005**, *5*, 5–9; e) H. Cho, B. R. Baker, S. Wachsmann-Hogiu, C. V. Pagba, T. A. Laurence, S. M. Lane, L. P. Lee, J. B. H. Tok, *Nano Lett.* **2008**, *8*, 4386–4390; f) H. Wang, C. S. Levin, N. J. Halas, *J. Am. Chem. Soc.* **2005**, *127*, 14992–14993; g) Q. Zhou, G. Zhao, Y. Chao, Y. Li, Y. Wu, J. Zheng, *J. Phys. Chem. C* **2007**, *111*, 1951–1954; h) H. Wang, J. Kundu, N. J. Halas, *Angew. Chem.* **2007**, *119*, 9358–9361; *Angew. Chem. Int. Ed.* **2007**, *46*, 9198–9202; i) A. Barhoumi, D. Zhang, F. Tam, N. J. Halas, *J. Am. Chem. Soc.* **2008**, *130*, 5523–5529.

[7] a) I. Yoon, T. Kang, W. Choi, J. Kim, Y. Yoo, S. W. Joo, Q. H. Park, H. Ihee, B. Kim, *J. Am. Chem. Soc.* **2009**, *131*, 758–762; b) T. Kang, I. Yoon, K. S. Jeon, W. Choi, Y. Lee, K. Seo, Y. Yoo, Q. H. Park, Y. Ihee, Y. D. Suh, B. Kim, *J. Phys. Chem. C* **2009**, *113*, 7492–7496; c) D. H. Jeong, Y. X. Zhang, M. Moskovits, *J. Phys. Chem. B* **2004**, *108*, 12724–12728; d) Y. P. Zhao, S. B. Chaney, S. Shanmukh, R. A. Dluhy, *J. Phys. Chem. B* **2006**, *110*, 3153–3157; e) A. Tao, F. Kim, C. Hess, J. Goldberger, R. He, Y. Sun, Y. Xia, P. Yang, *Nano Lett.* **2003**, *3*, 1229–1233; f) A. R. Tao, P. Yang, *J. Phys. Chem. B* **2005**, *109*, 15687–15690; g) L. Billot, M. L. de La Chapelle, A. S. Grimault, A. Vial, D. Barchiesi, J. L. Bijeon, P. M. Adam, P. Royer, *Chem. Phys. Lett.* **2006**, *422*, 303–307.

[8] a) S. Pierrat, I. Zins, A. Breivoge, C. Sönnichsen, *Nano Lett.* **2007**, *7*, 259–263; b) H. Wei, F. Hao, Y. Huang, W. Wang, P. Nordlander, H. Xu, *Nano Lett.* **2008**, *8*, 2497–2502; c) S. J. Lee, J. M. Baik, M. Moskovits, *Nano Lett.* **2008**, *8*, 3244–3247; d) J. A. Hutchison, S. P. Centeno, H. Odaka, H. Fukumura, J. Hofkens, H. Uji-i, *Nano Lett.* **2009**, *9*, 995–1001; e) Y. Fang, H. Wei, F. Hao, P. Nordlander, H. Xu, *Nano Lett.* **2009**, *9*, 2049–2053.

[9] a) A. J. Haes, R. P. V. Duyne, *J. Am. Chem. Soc.* **2002**, *124*, 10596–10604; b) N. H. Kim, S. J. Lee, K. Kim, *Chem. Commun.* **2003**, 724–725; c) N. P. W. Pieczonka, P. J. G. Goulet, R. F. Aroca, *J. Am. Chem. Soc.* **2006**, *128*, 12626–12627; d) K. K. Caswell, J. N. Wilson, U. H. F. Bunz, C. J. Murphy, *J. Am. Chem. Soc.* **2003**, *125*, 13914–13915.

[10] J. T. Golab, J. R. Sprague, K. T. Carron, G. C. Schatz, R. P. V. Duyne, *J. Chem. Phys.* **1988**, *88*, 7942–7951.

[11] a) K. Kim, J. K. Yoon, *J. Phys. Chem. B* **2005**, *109*, 20731–20736; b) W. Li, P. H. C. Camargo, X. Lu, Y. Xia, *Nano Lett.* **2009**, *9*, 485–490.

[12] a) M. Veiseh, B. T. Wickes, D. G. Castner, M. Zhang, *Biomaterials* **2004**, *25*, 3315–3324; b) S. Lan, M. Veiseh, M. Zhang, *Biosens. Bioelectron.* **2005**, *20*, 1697–1708.

Received: June 22, 2009
Revised: August 19, 2009
Published online: December 4, 2009

